Quantum Resistor-Capacitor Circuit with Majorana Fermion Modes in a Chiral Topological Superconductor

Minchul Lee[1] and Mahn-Soo Choi[2],*

[1]*Department of Applied Physics, College of Applied Science, Kyung Hee University, Yongin 446-701, Korea*
[2]*Department of Physics, Korea University, Seoul 136-701, Korea*

We investigate the mesoscopic resistor-capacitor circuit consisting of a quantum dot coupled to spatially separated Majorana fermion modes in a chiral topological superconductor. We find substantially enhanced relaxation resistance due to the nature of Majorana fermions, which are their own antiparticles and are composed of particle and hole excitations in the same abundance. Further, if only a single Majorana mode is involved, the zero-frequency relaxation resistance is completely suppressed due to a destructive interference. As a result, the Majorana mode opens an exotic dissipative channel on a superconductor which is typically regarded as dissipationless due to its finite superconducting gap.

As an electronic circuit is miniaturized on the nanometer scale, quantum coherence takes effect and transport properties get fundamentally different. For a ballistic conductor, Ohm's law breaks down and the conductance is quantized to multiples of $R_Q \equiv h/e^2$ [1,2], where h is the Planck constant and e is the electron charge. For a small resistor-capacitor circuit, the charge relaxation resistance is also quantized to $R_Q/2$, irrespective of the transmission properties [3,4], as demonstrated in an experiment on a quantum dot (QD) coupled to a quantum Hall edge channel [5]. The quantization is technically ascribed to the Fermi-liquid nature of the system [6–10], where the relaxation of particle-hole (*p-h*) pairs due to charge fluctuations at the cavity is the culprit for the dissipation. It is tempting and indeed customary [11] to interpret the quantized value as the contact resistance at a single interface (hence a half of the two-terminal contact resistance R_Q).

Here, we show that when the circuit involves Majorana fermions, which are casually regarded as half-fermions, the quantum resistance defies such an interpretation. Specifically, we examine a QD coupled, with different strengths, to two *spatially separated* one-dimensional (1D) chiral Majorana fermion modes; see Fig. 1. In the ultimate limit, a single Majorana mode is considered. The primary goal is to identify the role of each Majorana mode in relaxation resistance and compare it to the case of the Dirac fermion mode.

Mathematically, a Dirac fermion can always be decomposed into a pair of Majorana fermions, but these Majorana fermions usually occupy the same spatial location. However, the chiral topological superconductor (CTSC) states [12] enable the physical realization of spatially separated 1D Majorana fermion modes. An example is a quantum anomalous Hall (QAH) insulator proximity coupled to a conventional (or *normal*) superconductor (NSC) [12]. A HgTe quantum well doped with Mn [13] and a Bi_2Te_3 thin

film doped with Cr [14,15] turn into a QAH insulator with a chiral Dirac fermion edge mode, i.e., two chiral Majorana edge modes. When the QAH insulator is coupled to a NSC (see Fig. 1), the proximity-induced pairing potential pushes one of the two Majorana modes deeper into the bulk, spatially separating it from the other. As the relative magnitudes of the magnetization and the superconducting gap vary, the system undergoes topological phase transitions, from the QAH insulator phase to a CTSC phase (hereafter called the $CTSC_2$ phase) with two spatially separated Majorana edge modes [16], to another CTSC phase (called the $CTSC_1$ phase) with a single Majorana edge mode (one mode having disappeared into the bulk), and finally to a NSC without any edge channel [12].

Once the system enters the CTSC phases (either $CTSC_1$ or $CTSC_2$), we find that the low-frequency relaxation resistance is no longer pinned at $R_Q/2$ and strongly depends on the transmission properties. Especially, as the QD level approaches the resonance, the zero- or finite-frequency resistance is substantially enhanced, suggesting that Majorana modes boost the *p-h* pair generation and are highly dissipative. It contrasts with the gapped superconductor case, in which the resistance is suppressed
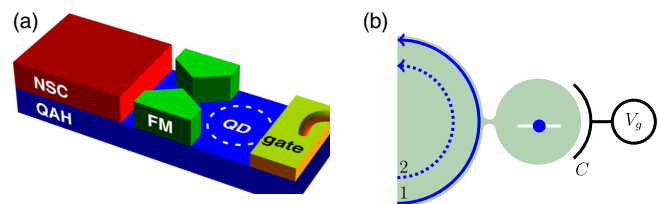
FIG. 1 (color online). (a) A possible realization of a quantum capacitor with spatially separated Majorana fermion modes. (b) A schematic of the coupling between two spatially separated Majorana edge modes ($j = 1, 2$) and the energy level localized on the QD.

for frequencies ω smaller than the gap. For the $CTSC_1$ phase with only a single Majorana edge mode, on the other hand, we find that the low-frequency relaxation resistance vanishes in the $\omega \to 0$ limit as for the fully gapped superconductor. The vanishing resistance is attributed to the exact cancellation between p-h pair generation processes in charge-conserving and pairing channels, as will be discussed later (see Fig. 3). These exotic behaviors are distinguished from those for normal superconductors or Dirac fermion channels. This casts an intriguing question about the role of the Majorana fermions in relaxation resistance and offers another method to probe the Majorana fermions.

Model.—Focusing on the low-energy physics inside the bulk gap, one can describe a CTSC with two chiral Majorana modes

$$H_{\text{Majorana}} = \sum_{j=1,2} \sum_{k>0} \epsilon_k \gamma_{-k,j} \gamma_{k,j}, \qquad (1)$$

where $\gamma_{k,j} = \gamma_{-k,j}^\dagger$ are chiral Majorana fermion operators, $\epsilon_k = \hbar v k$ is their energy, and v is the propagation velocity of the Majorana edge modes. In the $CTSC_1$ phase, we regard the mode $j = 2$ disappearing into the bulk.

The QD can be formed by depositing ferromagnetic insulators (FMs), which turn the underneath region into the trivially insulating state (I). A proper placement of FMs deforms and localizes the QAH edge states to form a QD; see Fig. 1(a). Since the localized state in the QD originates from the spin-polarized QAH edge state, it is described as a single spinless level ϵ_d:

$$H_{\text{QD}} = \{\epsilon_d + e[U(t) - V_g(t)]\} n_d. \qquad (2)$$

Here, $n_d = d^\dagger d$ is the occupancy operator, and the ac voltage $V_g(t)$ upon the gate coupled to the QD via a geometrical capacitance C induces the polarization charge on the dot and eventually the internal potential $U(t)$. The latter is determined self-consistently under the charge conservation condition.

The coupling of the QD level to the chiral Majorana edge modes ($j = 1, 2$) takes a tunneling model [17]

$$H_{\text{tun}} = \sum_k [t_1 d^\dagger \gamma_{k,1} + i t_2 d^\dagger \gamma_{k,2} + (\text{H.c.})]. \qquad (3)$$

Here, for simplicity, we have assumed wide bands and neglected the momentum dependence of the tunneling amplitudes t_j between the Majorana mode j and the QD level. In this limit, the coupling is conveniently described by the hybridization parameters $\Gamma_j \equiv |t_j|^2/\hbar v$ ($\sim$0.4–4 μeV [5]) and $\Gamma_\pm \equiv (\Gamma_2 \pm \Gamma_1)/2$. In general, $\Gamma_1 \geq \Gamma_2$ due to their spatially separated localizations; in particular, $\Gamma_2 = 0$ in the $CTSC_1$ phase and $\Gamma_1 = \Gamma_2$ only in the QAH phase. Note that our model ignores the bulk states of the reservoir and Γ_1 and ω should be sufficiently smaller

than the bulk gap; it is inadequate when the system is too close to the $CTSC_2$-$CTSC_1$ transition point, where the bulk gap is small. Γ_2 may vanish well before the transition point due to the exponential suppression with the distance of the tunneling.

Relaxation resistance.—We calculate the ac current $I(t)$ between the reservoir of Majorana modes and the QD or, equivalently, the displacement current between the top gate and the QD, using the self-consistent mean-field approach in the linear-response regime [3,4,6–10,18] (see Ref. [19], Secs. II A and B). The relaxation resistance $R_q(\omega)$ is then obtained from its relation to the admittance $g(\omega)$ $[1/g(\omega) = R_q(\omega) + i/\omega C_q(\omega)]$, where $C_q(\omega)$ is the quantum correction to the capacitance. At zero temperature, the admittance allows for a closed-form expression and reads as (hereafter, we set $\hbar = k_B = 1$)

$$g(\omega) = \frac{1}{R_Q} \sum_{\mu=\pm} \left\{ \frac{\Gamma_-^2}{\varepsilon(\omega + \mu\varepsilon)} \ln \frac{\Gamma_+ + i\varepsilon}{\Gamma_+ - i\varepsilon} \right.$$
$$\left. + \left[\frac{\Gamma_-^2}{\varepsilon(\varepsilon + \mu\omega)} + \frac{\Gamma_+}{\Gamma_+ + i\omega} \right] \ln \frac{\Gamma_+ + i(2\omega + \mu\varepsilon)}{\Gamma_+ + i\mu\varepsilon} \right\}, \qquad (4)$$

with $\varepsilon \equiv \sqrt{4\epsilon_d^2 - \Gamma_-^2}$. Equation (4) is the main result of this work. We now discuss its physical implications.

Zero-frequency resistance at zero temperature.—Let us first focus on the zero-frequency limit ($\omega \ll \epsilon_d^2/\Gamma_1$) of the resistance $R_0 \equiv R_q(\omega \to 0)$; see Fig. 2 and Ref. [19], Sec. II C. In the QAH phase, where the two Majorana modes equally contribute ($\Gamma_1 = \Gamma_2$), the resistance restores the quantized value $R_0 = R_Q/2$, as expected, because the two Majorana modes in the QAH phase are equivalent to a single Dirac fermion mode.

As the system evolves into the $CTSC_2$ phase ($0 < \Gamma_2 < \Gamma_1$), R_0 does not only deviate from the quantized
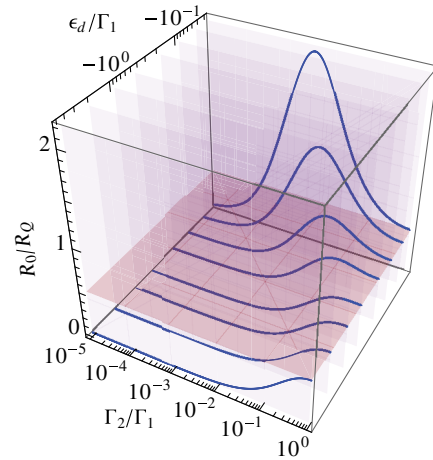
FIG. 2 (color online). Zero-frequency relaxation resistance $R_0 = R_q(\omega \to 0)$ as a function of ϵ_d and Γ_2. For comparison, a shaded horizontal surface is also drawn at the quantized value $R_Q/2$.

value but also depends on the ratio Γ_2/Γ_1 and the QD level ϵ_d, as shown in Fig. 2. When the dot level is far from the resonance ($|\epsilon_d| \gg \Gamma_1$), the zero-frequency resistance $R_0 \approx (R_Q/2)[4(\Gamma_2/\Gamma_1)/(1 + \Gamma_2/\Gamma_1)^2]$ depends only and monotonically on the ratio Γ_2/Γ_1; see the curve for large values of $|\epsilon_d|$ in Fig. 2. When the dot level resonates with the Fermi level ($|\epsilon_d| \ll \Gamma_1$), it now depends nonmonotonically on Γ_2/Γ_1 with the maximum at $\Gamma_2 \approx \Gamma_m \equiv 4\epsilon_d^2/\Gamma_1$ of the height $\sim [4\gamma_m \ln \gamma_m]^{-1}$ with $\gamma_m \equiv \Gamma_m/\Gamma_1$. In short, unlike the Dirac fermion case, R_0 for the reservoir of Majorana modes strongly depends on the properties of the tunneling barrier and the QD and thus defies the simple interpretation [11] of it as a half of the two-terminal contact resistance.

The zero-frequency relaxation resistance in the CTSC$_1$ phase with a single Majorana mode ($\Gamma_2 = 0$) is even more interesting and exotic: it vanishes exactly $R_0 = 0$, irrespective of Γ_1, Γ_2, and ϵ_d, although there is no excitation energy gap (see Ref. [19], Sec. II C). To understand it, we introduce chiral Dirac fermion operators $c_k \equiv (\gamma_{k,1} + i\gamma_{k,2})/\sqrt{2}$ composed of the two Majorana fermions, in terms of which the Hamiltonians (1) and (3), respectively, are rewritten as

$$H_{\text{Majorana}} = \sum_k \epsilon_k c_k^\dagger c_k, \tag{5}$$

$$H_{\text{tun}} = \sum_k [t_{\text{single}} d^\dagger c_k + t_{\text{pair}} d^\dagger c_k^\dagger + (\text{H.c.})], \tag{6}$$

with $t_{\text{single(pair)}} \equiv (t_1 \pm t_2)/\sqrt{2}$. This form (6) immediately suggests two distinctive types of processes, as illustrated in Fig. 3: One is the charge-conserving type from the t_{single} term, in which the p-h pair is excited via the electron tunneling in and out of the QD [Fig. 3(a)]. This type of process alone would give rise to $R_0 = R_Q/2$ [7–10]. The other is a pairing type involving the t_{pair} term which accompanies the creation and destruction of a Cooper pair in the bulk [Fig. 3(b)]. This type is missing in the QAH phase, where $t_1 = t_2$. When the QD is initially occupied, the charge-conserving (pairing) process creates the particle (hole) first. Hence, the p-h pair amplitudes of the two processes are opposite in sign (at all orders) due to the fermion ordering. When $\Gamma_2 = 0$ ($t_{\text{single}} = t_{\text{pair}}$), both types are the same in magnitude, so as to cancel out each other exactly. This cancellation and the subsequent vanishing resistance are hallmarks of the relaxation via the Majorana modes. Note, however, that this cancellation is exact only for $\Gamma_2 = 0$ and for p-h pairs with vanishingly small energy (the $\omega \to 0$ limit). At finite ω, as shown below, the intermediate virtual states are different for two processes so that the cancellation is not perfect.
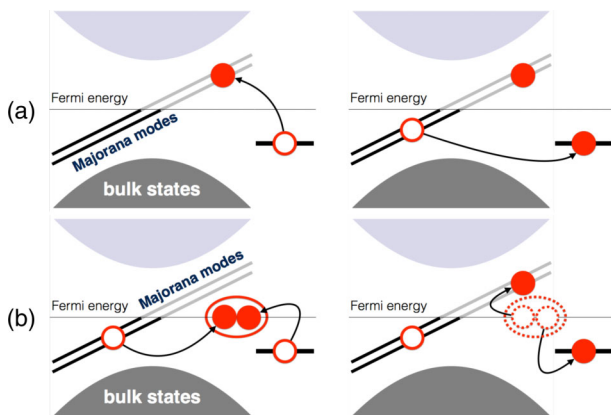
Finite-frequency resistance at zero temperature.—We find that the vanishing or enhancement of the resistance discussed above becomes even more pronounced at finite frequencies. While the finite-frequency resistance $R_q(\omega)$ is 0 for a conventional superconducting reservoir or even for Andreev bound states localized at yet propagating along its edge (Andreev edge modes) due to their finite gap (see Ref. [19], Sec. III D), it grows with $|\omega|$ for the gapless Dirac fermion reservoir since the spectral density of p-h excitations grows with energy [7]. In the QAH phase, $R_q(\omega)$ grows slowly and monotonically with ω [Fig. 4(a)]. Entering the CTSC phase, however, $R_q(\omega)$ becomes highly nonmonotonic, forming an ever narrower dip at $\omega = 0$, and peaks at $|\omega| \sim \Gamma_m$ [Figs. 4(a) and 4(b)]. The dip width is the order of Γ_m for $\Gamma_2 \approx 0$.

FIG. 3 (color online). Second-order processes to generate a p-h pair in the Majorana fermion channel via (a) the charge-conserving process ($\sim |t_{\text{single}}|^2$) and (b) the pairing process ($\sim |t_{\text{pair}}|^2$) when the QD is initially occupied. The degenerate Majorana modes are artificially split here as a guide for the eye.
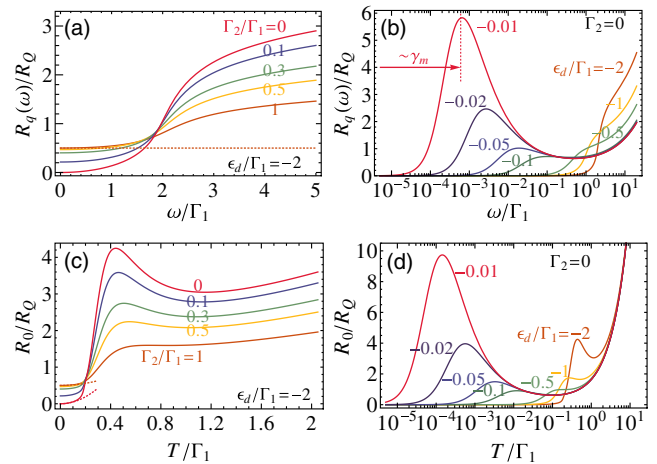
FIG. 4 (color online). (a),(b) Zero-temperature resistance $R_q(\omega) = R_q(-\omega)$ as a function of frequency ω. (c),(d) Zero-frequency resistance R_0 as a function of temperature T. $\epsilon_d/\Gamma_1 = -2$ in (a) and (c), and $\Gamma_2 = 0$ in (b) and (d). The arrow in (b) indicates the approximate peak position $\sim \gamma_m$ for $\Gamma_2 = 0$ and $\epsilon_d/\Gamma_1 = -0.01$. The dotted lines in (c) correspond to the low-temperature asymptotes.

Let us examine the CTSC$_1$ phase ($\Gamma_2 = 0$) in three different regimes: the (i) off-resonance ($|\epsilon_d| \gg \Gamma_1$), (ii) near-resonance ($0 < |\epsilon_d| \ll \Gamma_1$), and (iii) exact-resonance ($\epsilon_d = 0$) regimes. (i) In the off-resonance regime, the resistance grows like $R_q(\omega) \approx (R_Q/3)(\omega/\epsilon_d)^2$ for small frequencies ($\omega \ll \Gamma_m$) and keeps growing monotonically for higher frequencies. Note that in this limit, the resistance is independent of the barrier transmission. (ii) In the near-resonance regime, $R_q(\omega) \approx t[R_Q/3\gamma_m(\ln \gamma_m)^2](\omega/\Gamma_m)^2$ for $\omega \ll \Gamma_m$, and it shows sharp peaks at $\omega \approx \pm\Gamma_m$ [Fig. 4(b)]. The quadratic growth and dip-peak structure around $\omega = 0$ cast stark contrasts with the superconducting reservoir or the case with Andreev edge modes; in the latter case, the peak is either pinned at the gap energy or linearly dependent on the QD level (see Ref. [19], Sec. III E). (iii) Even more dramatic contrast appears at the exact resonance. In this case, the two peaks at $\omega \approx \pm\Gamma_m$ in Fig. 4(b) merge together, filling up the dip at $\omega = 0$ (i.e., the dip width is 0). As a result, the resistance $R_q(\omega) \approx \pi R_Q/4(2|\omega|/\Gamma_1)[\ln(2|\omega|/\Gamma_1)]^2$ diverges as $\omega \to 0$. In summary, the finite-frequency relaxation resistance is genuinely enhanced for $\Gamma_2 \ll \Gamma_1$ near resonance.

All-Majorana representation.—To understand the enhancement of the resistance near resonance, it is instructive to describe the dot level in terms of the language of Majorana fermions as well (see Ref. [19], Sec. II D). We define two Majorana operators $\gamma_{d,j}$ ($j = 1, 2$) by $\gamma_{d,1} = (d - d^\dagger)/\sqrt{2}i$ and $\gamma_{d,2} = (d + d^\dagger)/\sqrt{2}$. Unlike the Majorana fermions on the edge modes of the CTSC, these dot Majorana fermions are rather mathematical, as they occupy the same spatial location. The QD and coupling Hamiltonians (2) and (3), respectively, read as

$$H_{\text{QD}} = i\epsilon_d \gamma_{d,2} \gamma_{d,1}, \tag{7a}$$

$$H_{\text{tun}} = \sum_k i(t_2 \gamma_{d,2} \gamma_{k,2} - t_1 \gamma_{d,1} \gamma_{k,1}). \tag{7b}$$

In this expression, ϵ_d becomes the coupling between the two dot Majorana fermions. The two Majorana edge modes in the reservoir are coupled *indirectly* via the coupling between two Majorana fermions on the dot, being completely decoupled at the resonance ($\epsilon_d = 0$). However, it does not mean that their contributions are independent [see Eq. (8) below] because the charge is always composed of two Majorana fermions. At $\epsilon_d = 0$, the real part of admittance, representing the dissipation, is expressed as

$$\text{Re}[g(\omega)] = \frac{2\pi^2}{R_Q} \omega \int_0^\omega d\omega' \rho_1(\omega - \omega')\rho_2(\omega'), \tag{8}$$

where $\rho_i(\omega')$ is the density of states for $\gamma_{d,i}$, which is Lorentzian, centered at $\omega' = 0$ and with width Γ_i. If both ρ_1 and ρ_2 are finite, then $\text{Re}[g(\omega)] \sim \omega^2$ for $\omega \to 0$, so that R_0 is finite; recall that $g(\omega) \approx -i\omega C_q + \omega^2 C_q^2 R_0$. However, as

$\Gamma_2 \to 0$, $\rho_2(\omega')$ becomes sharper, and eventually, $\rho_2(\omega') = \delta(\omega')$ at $\Gamma_2 = 0$, so that $\text{Re}[g(\omega)] \sim \omega$, i.e., $R_0 \propto 1/\omega$, as seen above. In short, the resistance enhancement at resonance is attributed to a decoupled dot Majorana with an abundant density of states near zero energy; the dot *electron* is coupled equally to the particle and hole components of the single Majorana edge mode so that the Majorana nature, leading to a proliferation of *p-h* pairs, is highly pronounced. A single local Majorana fermion coupled to a chiral Majorana line has appeared in a different context, essentially a two-channel Kondo model, and a similar divergence $R_q \sim 1/\omega(\log \omega)^2$ has been observed [27]. This suggests that the exotic behaviors of our system may be a non-Fermi-liquid feature.

For $\epsilon_d \neq 0$, $\gamma_{d,1}$ and $\gamma_{d,2}$ are coupled and interfere with each other, causing anti-Fano-like destructive interference: The broadening of $\gamma_{d,2}$ is $\sim\Gamma_m$, and the destructive interference leads to a dip in $\rho_1(\omega)$ of width $\sim\Gamma_m$ (Fig. 4). This is another explanation, now based on the interference between Majorana fermions, of the vanishing low-frequency resistance discussed before.

Decoherence effects.—We remark that all the features discussed so far—the vanishing low-frequency resistance and the divergence of the resistance *at resonance*—occur only when the full coherence is maintained. In the presence of decoherence, the resistance would deviate from those coherent values. For example, when the dot is subject to random background charge fluctuations, which are the most common decoherence source on QDs, it leads to the fluctuation in ϵ_d. In effect, it pushes the system away from the resonance and the resistance does not diverge. Another indication of decoherence effects can be seen in the finite-temperature effect discussed below.

Finite-temperature effect.—Typically, R_q increases with temperature T since the thermal fluctuations promote the generation of *p-h* pairs [6]. For $T \ll \Gamma_m$, the Sommerfeld expansion (see Ref. [19], Sec. II E) gives rise to $R_0 \approx R_0|_{T=0} + R_Q(2\pi^2/3)(T/\epsilon_d)^2(1 + \Gamma_-^2/\Gamma_+^2)$ in the off-resonance regime [Fig. 4(c)]. For higher temperatures, however, nonmonotonic behavior is observed for $\Gamma_2 \ll \Gamma_1$ [Fig. 4(d)]: A peak occurs at $T \sim \Gamma_m$, whose height grows as $|\epsilon_d|$ decreases. The enhancement of R_q around this particular temperature is related to the peak structure in zero-temperature $R_q(\omega)$ located at $\omega \sim \Gamma_m$, as shown in Fig. 4(b). In the presence of thermal fluctuations, the contribution of low-energy *p-h* pairs that are suppressed due to the destructive interference between $\gamma_{d,1}$ and $\gamma_{d,2}$ decreases. Instead, the *p-h* pairs, which have energy $\sim\Gamma_m$ and are not affected by the cancellation, cause the surge of the resistance. Together with the nonmonotonic frequency dependence of $R_q(\omega)$, the peak structure driven by the thermal excitations is a unique feature of dissipation via Majorana states.

*choims@korea.ac.kr

[1] B. J. van Wees, H. van Houten, C. W. J. Beenakker, J. G. Williamson, L. P. Kouwenhoven, D. van der Marel, and C. T. Foxon, Phys. Rev. Lett. **60**, 848 (1988).

[2] D. A. Wharam, T. J. Thornton, R. Newbury, M. Pepper, H. Ahmed, J. E. F. Frost, D. G. Hasko, D. C. Peacock, D. A. Ritchie, and G. A. C. Jones, J. Phys. C **21**, L209 (1988).

[3] M. Büttiker, H. Thomas, and A. Prêtre, Phys. Lett. A **180**, 364 (1993).

[4] M. Büttiker, A. Prêtre, and H. Thomas, Phys. Rev. Lett. **70**, 4114 (1993).

[5] J. Gabelli, G. Fève, J.-M. Berroir, B. Plaçais, A. Cavanna, B. Etienne, Y. Jin, and D. C. Glattli, Science **313**, 499 (2006).

[6] S. E. Nigg, R. López, and M. Büttiker, Phys. Rev. Lett. **97**, 206804 (2006).

[7] M. Lee, R. López, M.-S. Choi, T. Jonckheere, and T. Martin, Phys. Rev. B **83**, 201304 (2011).

[8] C. Mora and K. Le Hur, Nat. Phys. **6**, 697 (2010).

[9] M. Filippone, K. Le Hur, and C. Mora, Phys. Rev. Lett. **107**, 176601 (2011).

[10] H. Khim, S.-Y. Hwang, and M. Lee, Phys. Rev. B **87**, 115312 (2013).

[11] M. Büttiker, J. Korean Phys. Soc. **34**, S121 (1999).

[12] X.-L. Qi, T. L. Hughes, and S.-C. Zhang, Phys. Rev. B **82**, 184516 (2010).

[13] C.-X. Liu, X.-L. Qi, X. Dai, Z. Fang, and S.-C. Zhang, Phys. Rev. Lett. **101**, 146802 (2008).

[14] R. Yu, W. Zhang, H.-J. Zhang, S.-C. Zhang, X. Dai, and Z. Fang, Science **329**, 61 (2010).

[15] C.-Z. Chang, J. Zhang, X. Feng, J. Shen, Z. Zhang, M. Guo, K. Li, Y. Ou, P. Wei, L.-L. Wang et al., Science **340**, 167 (2013).

[16] To be precise, the QAH and CTSC$_2$ phases are topologically indistinguishable. The distinction is just for convenience.

[17] R. Žitko, Phys. Rev. B **83**, 195137 (2011).

[18] A.-P. Jauho, N. S. Wingreen, and Y. Meir, Phys. Rev. B **50**, 5528 (1994).

[19] See Supplemental Material at http://link.aps.org/supplemental/10.1103/PhysRevLett.113.076801, which includes Refs. [3,4,6,10,12,17,18,20–26], for technical details and the comparison with Adnreev edge modes.

[20] N. S. Wingreen, A.-P. Jauho, and Y. Meir, Phys. Rev. B **48**, 8487 (1993).

[21] A. F. Andreev, Sov. Phys. JETP **22**, 455 (1966).

[22] A. V. Shytov, P. A. Lee, and L. S. Levitov, Phys. Usp. **41**, 207 (1998).

[23] A. F. Volkov, P. H. C. Magnée, B. J. van Wees, and T. M. Klapwijk, Physica (Amsterdam) **242C**, 261 (1995).

[24] N. Read and D. Green, Phys. Rev. B **61**, 10 267 (2000).

[25] M. Sato and S. Fujimoto, Phys. Rev. B **79**, 094504 (2009).

[26] P. G. de Gennes, Superconductivity of Metals and Alloys (Westview, New York, 1999).

[27] C. Mora and K. Le Hur, Phys. Rev. B **88**, 241302 (2013).